International Journal of Biological Macromolecules 211 (2022) 218–229

Contents lists available at ScienceDirect

International Journal of Biological Macromolecules

journal homepage: www.elsevier.com/locate/ijbiomac

Composites of cellulose nanocrystals in combination with either cellulose nanofibril or carboxymethylcellulose as functional packaging films

Julia Fernández-Santos, Cristina Valls, Oriol Cusola, M. Blanca Roncero *

CELBIOTECH_Paper Engineering Research Group, Universitat Politècnica de Catalunya_BarcelonaTech, 08222 Terrassa, Spain

ARTICLE INFO

Keywords:
Nanocellulose
Carboxymethylcellulose
Barrier properties
Food packaging

ABSTRACT

Cellulose nanocrystals (CNC) were mixed with either cellulose nanofibril (CNF) or carboxymethylcellulose (CMC) in variable proportions (0/100, 20/80, 40/60, 50/50, 60/40, 80/20 and 100/0) to obtain cast films with acceptable barrier and mechanical properties as replacements for food packaging plastics. Both CNF and CMC improved tensile strength, elongation, UV opacity, air resistance, hydrophobicity (WCA-water contact angle), water vapor transmission rate (WVTR) and oxygen impermeability in pure CNC. WVTR and oxygen permeability were strongly dependent on relative humidity (RH). Interestingly, the greatest effect on WVTR was observed at RH = 90% in films containing CMC in proportions above 60%. CMC- and CNF-containing films had oxygen impermeability up to an RH level of 80% and 60%, respectively. The previous effects were confirmed by food packaging simulation tests, where CMC-containing films proved the best performers. The composite films studied were biodegradable—which constitutes a major environmental related advantage—to an extent proportional to their content in CMC or CNF.

1. Introduction

Natural biopolymers are being increasingly used as replacements for petroleum derivatives worldwide in order to address serious environmental and health problems of which scientists and society at large are well aware [1]. Developing effective alternatives to troublesome materials is the focus of much current research in various scientific areas including food technology and, especially, food packaging. For a long time now, foods have been stored in plastic materials, which have been the source of deleterious effects on health and the environment [2,3]. Plastics have so far been used for this purpose on the grounds of their wide availability in large amounts, their good tensile strength and their low oxygen permeability. Unfortunately, they are not biodegradable, which has become not only a functional requirement but also a major attribute of environmental friendliness for the packaging industry [4]. Extending the shelf life of foods while preserving their quality—or even improve it—is essential, but so is protecting the environment by using renewable, recyclable and biodegradable materials for packaging. In this scenario, natural biopolymers may provide an effective choice for developing environmentally safe packaging materials with good barrier and mechanical properties.

Cellulose is one of the most abundant natural biopolymers. This has boosted its massive use by the paper, textile, food, pharmaceutical and veterinary industries, among others [5,6]. In recent decades, however, cellulose has started to be increasingly used as a replacement for petroleum derivatives. In fact, cellulose derivatives—and, more recently, nanocellulose—have aroused increasing interest in the food industry by virtue of their good barrier properties [7,8], and also of their recyclability and biodegradability [9]. Food packaging helps to store and preserve (nutritional and organoleptic) properties of food, not only preserving it from spoilage, but also protecting it from physical and environmental conditions [10]. There are many studies on nanopackaging in the food industry. This industry is one of the sectors where nanotechnology has transformed the way food is preserved and packaged. However, only a few works have focused on new generation packaging that encourages the use of natural polymers to replace traditional plastics [3]. Although they may be effective alternatives to existing plastics, their high sensitivity to moisture must be lessened

Abbreviations: CNC, cellulose nanocrystals; CNF, cellulose nanofibril; CMC, carboxymethylcellulose; RH, relative humidity; WCA, water contact angle; WDT, water drop test; OP, Oxygen permeability; WVTR, Water vapor transmission rate.

* Corresponding author.
E-mail addresses: julia.fernandez.santos@upc.edu (J. Fernández-Santos), cristina.valls@upc.edu (C. Valls), oriol.cusola@upc.edu (O. Cusola), blanca.roncero@upc.edu (M.B. Roncero).

https://doi.org/10.1016/j.ijbiomac.2022.05.049
Received 31 January 2022; Received in revised form 4 May 2022; Accepted 6 May 2022
Available online 11 May 2022

before they can be effectively used as packaging materials [11]. Nanocellulose can be obtained from plants, bacteria or tunicates, being more commonly obtained from plants, including cotton, cotton linters, kenaf fiber, wheat straw, and wood fiber [12,13]. The properties of nanocellulose vary slightly with origin. Thus, bacterial nanocellulose is highly crystalline, whereas vegetable nanocellulose typically occurs as nanocrystals (CNC) or nanofibers (CNF).

The process to obtain CNC involves hydrolysis, usually with sulfuric acid, of the amorphous portion of cellulose, giving rise to crystalline cellulose nanostructures [14,15]. CNC displays rod-like structure (5–30 nm in diameter and 100–500 nm in length) with larger specific surface area and high crystallinity [16]. On the other hand, CNF have a large specific surface area (10–100 nm in diameter, 1–10 μm in length) and are typically obtained by high-shear mechanical disintegration of cellulose fibers with an enzymatic or chemical pretreatment and contain both crystalline and amorphous cellulose parts [17].

CNC is very interesting for application in the food packaging industry because it produces transparent films and has the advantage of being less moisture-sensitive due to its higher crystallinity than CNF [18]. However, this higher crystallinity has also the disadvantage of producing films that are much more fragile and difficult to handle. Fernández-Santos et al. [19] observed low barrier and mechanical properties of CNC films, and concluded that it was necessary to add additives to improve these properties. They also found that the addition of natural additives such as sorbitol was needed to preserve the oxygen impermeability until a relative humidity (RH) of 70%.

Although CNF has very good mechanical properties and oxygen impermeability, their barrier properties degrade heavily with increasing moisture [7] and the resulting films do not possess good transparency [20]. Very few studies have compared barrier properties in CNC and CNF; also, most have used them as paper coatings rather than pure films [7,21–24].

Carboxymethylcellulose (CMC) is a water-soluble cellulose derivative containing carboxymethyl (CH_2COOH) groups and hydroxyl groups in the cellulose chain [25]. By virtue of its physicochemical and biological properties, CMC has been used as an oxygen- and carbon dioxide-barrier material [8]. CMC is used as a food additive to provide stability and thickness to foods, due its high viscosity at relatively low concentration [26]. In addition, it has been widely used among cellulose derivatives to prepare biodegradable films due to its biodegradability and biocompatibility [17]. CMC has good film-forming properties, with high optical transparency and high chemical stability [27,28]. Unfortunately, CMC films have poorer mechanical properties than other cellulose-based films as a result of their being adversely affected by moisture [8,17].

Tavares et al. [29] found that CMC exhibited better properties when mixed with starch. Oun & Rhim [30,31] previously found mixing CMC with 5% CNF or 5% CNC to improve the properties of the starting material. Although CNC, CNF and CMC possess some interesting characteristics to be applied as packaging materials, they have a lack of some mechanical and barrier properties. Thus, the starting hypothesis for this work was that mixing CNC with either CNF and CMC could allow fully functional films to be obtained through a synergistic combination of their properties. For example, because CMC seemingly possesses very good oxygen-barrier properties [8], its addition to CNC was expected to improve packaging performance in its films and to make them suitable for the intended purpose as a result. In fact, no study spanning the whole possible range of CMC proportions in combination with CNC appears to have been reported to date.

Therefore, in this work, we mixed CNC with variable proportions of either CNF or CMC to obtain composite films with high transparency and also with barrier, structural, mechanical, optical and morphological properties similar to petroleum-derived materials. These more sustainable films could be used as functional, environmentally safe packaging materials by the food industry. CNC was selected as the basis film because of the optical transparency it can provide to the final films, and also since high solids formulations are possible with mainly CNC, due to its uniformity of particle dimensions and moderate aspect ratio.

Work toward this goal was conducted in two parts. One involved constructing and characterizing CNC films containing variable proportions of CNF, and assessing whether the resulting improvements in barrier properties overcame the wettability, hydrophobicity and oxygen-barrier shortcomings of CNF at a high relative humidity. The other part involved constructing and characterizing CNC–CMC composite films. CNC–CNF and CNC–CMC composite films were examined in morphological and structural terms, as well as for optical and mechanical properties, and for biodegradability. In addition, they were subjected to a test mimicking real-life packaging conditions for food (olives).

2. Materials and methods

2.1. Materials

Cellulose nanocrystals (CNC) and cellulose nanofibril (CNF) provided by University of Maine (Maine, United States) were used as main raw materials. Isopropyl alcohol ($CH_3CHOHCH_3$, 99.8%, Lot number: 0000741157), sodium hydroxide (NaOH, 100%, Lot number: 0000975387), methanol (CH_3OH, 99.5%, Lot number: 0000688234), acetic acid (CH_3COOH, 99.9%, Lot number: 0000957900) and ethanol (CH_3CH_2OH, 99.8%, Lot number: 0001976879) were purchased from PanReac AppliChem (Germany). Monochloroacetic acid ($C_2H_3ClO_2$, 100%, Lot number: S6928112538) was purchased from Merck kGaA (Germany). Cotton linters were obtained from Celesa (Celulosa de levante, s.a., Spain).

2.2. Carboxymethylcellulose (CMC)

2.2.1. Synthesis of CMC

The CMC was prepared following the method described by Browning [32]. 15 g of cotton linters were mixed with 400 ml of isopropyl alcohol in a beaker. After 30 min with vigorous mechanical stirring, 50 ml of a 40% (v/v) aqueous solution of sodium hydroxide were added and, over a period of 1 h at room temperature, stirring was continued. Chloroacetic acid (18 g) was then added over a period of 30 min. The beaker was covered with aluminum foil and placed in an oven at 55 °C for 3.5 h. After heating, the solution was separated into two layers. The upper liquid layer was discarded and the lower solid phase was dispersed in 300 ml of methanol 70% (v/v) and neutralized with 90% (v/v) acetic acid. The fibers were separated by filtration, stirred into 70% (v/v) ethanol (300 ml) and allowed to stand for 10 min. The filtration and stirring with ethanol are repeated six times, after which the fibers were washed with absolute methanol and dried at 60 °C. The product should be a degree of substitution $\leq$1.

2.2.2. Determination of the degree of substitution (DS) of CMC

5 measurements were performed for this analysis. 5 g of CMC was added to 200 ml HNO_3-methanol (1:1 v/v). This solution was shaken for 3 h. The excess of acid was washed with a 70% (v/v) methanol solution. After drying CMC overnight at 60 °C, 2 g of dried sample was dissolved in 200 ml of distilled water and 30 ml of 1 N NaOH mixture. Then, the solution was titrated by 1 N HCl. The DS of CMC was determined by following equations [33,34]:

$$DS = \frac{0.162*A}{[1-(0.058*A)]} \quad (1)$$

$$A = \frac{(B*C)-(D*E)}{F} \quad (2)$$

where:

A: equivalent weight of alkali required per gram of CMC

B: amount of NaOH solution (ml)

C: normality of NaOH solution (N)
D: amount of HCl solution (ml)
E: normality of HCl solution (N)
F: weight of CMC (g).

2.3. Preparation of films by casting method

In order to obtain films with advanced properties, it was mixed CNC/CMC, and CNC/CNF to obtain films by casting method at the proportions of 0/100, 20/80, 40/60, 50/50, 60/40, 80/20 and 100/0 (Fig. S1 in Supplementary data). The mixtures were prepared by adding the necessary water to obtain a final consistency of 2%. For correct homogenization, the mixture between CNC and CMC was stirred with vigorously shaking (700 rpm) for 1 h; and the mixture between CNC and CNF was sonicated for 20 min on an ultrasound tip with 50% of amplitude (Branson™). The suspensions were deposited on a polystyrene plastic surface and allowed to evaporate at controlled humidity (50% RH) and temperature (23 °C) conditions, for about 5 days.

2.4. Characterization of films

2.4.1. Structural properties

Thickness, basis weight and density were measured according to ISO 534:2011. Roughness of the films was measured following the ISO 8791-2:2013 standard. Surface and cross sections of the films were observed by SEM (JSM 7100 F) using a LED filter. All the samples were graphite coated using EMITECH K950X221.

2.4.2. Optical properties

The absorbance was measured at room temperature in steps of 1 nm, in the range of 200 to 900 nm with an Evolution 600 UV–visible spectrophotometer. Transmittance of the film at 600 nm was also measured. The transparency of the films was calculated from the percent transmittance of light at 600 nm, following the eq. 3 [35]:

$$Transparency = \left(\frac{-log\%T600}{x}\right) \quad (3)$$

where %T600 is the percent transmittance at 600 nm and x is the film thickness (mm).

2.4.3. Mechanical properties

Mechanical properties of the films such as tensile strength, elongation at break and Young's modulus was carried out by using a Metrotec-quality control instruments T5K equipped with a 500 N load cell. The films were cut into rectangular shape with 15 mm width and 50 mm length.

2.4.4. Barrier properties

Air permeance was measured following the standard ISO 5636-3:2013. Water absorption was evaluated using an adaptation of the TAPPI T835, in which a drop of water is deposited on the surface of film and then it is measured the time that it took to disappear the specular gloss of the drop of water. The hydrophobicity was measured by the water contact angle (WCA) using a Dataphysics OCA15EC contact angle goniophotometer with an image capture ratio of 25 frame/s. A 4 μl water drop was delivered to sample surface and at least 5 measurements were made for each film. Since 5 films were produced for each condition, 10 measures of WCA were performed by sample. Oil resistance was measured in accordance with the standard ISO 16532-3:2010, following the turpentine test. Oxygen permeability was measured using MOCON OX-TRAN® Model 1/50 with an atmospheric oxygen concentration of 100% at 23 °C temperature and at different relative humidity (0, 20, 40, 60, 70, 80 and 90%). Water vapor transmission rate (WVTR) of the films was measured according to the standard procedure ISO 2528 (2017) at 25 °C and 50% and 90% RH. The procedure was carried out as follows: an aluminum cup containing $CaCl_2$ desiccant was sealed by the test film (50 cm^2 exchange film area) with paraffin wax at 90 °C and placed in a climatic chamber for controlling the environmental conditions. All tests were performed in duplicate. The WVTR (g m^{-2} day^{-1}) was determined using the eq. 4:

$$WVTR = \frac{m*24*10^4}{S*t} \quad (4)$$

where m is the increase in mass, in grams, of the assembly during the time t; S is the area of the tested surface of the test piece and t is the total duration, in hours, of the last two stable exposure periods.

2.4.5. FTIR spectroscopy

FTIR spectra of CNC films were recorded in duplicate at room temperature using an ATR-FTIR spectrophotometer (Spectrum 100, Perkin Elmer, USA). FTIR spectral analyses were conducted within the wavenumber range of 500–4000 cm^{-1}. A total of 64 scans were run to collect each spectrum at a 1 cm^{-1} resolution.

2.4.6. X-ray diffraction (XRD)

CNC films were subjected to X-ray diffractometry analysis (PANalytical X'Pert PRO MPD Alpha1 powder diffractometer in a Bragg-Brentano θ/2θ geometry of 240 mm of radius). The samples were analysed at the radiation wavelength of 1.5406 Å and 45 kV–40 mA for the work power. Samples were scanned from 2 to 60°, 2Θ range. The samples were mounted with no support fixed by mean of two polyoxymethylene rings, and analysed in reflection geometry. The crystallinity index (CI) was calculated based on Eq. (5) [36].

$$CrI(\%) = \frac{I_c - I_{am}}{I_c} \times 100 \quad (5)$$

where I_c is the maximum intensity of the lattice diffraction and I_{am} is the intensity of the peak at $2\Theta = 18°$, which corresponds to the amorphous part of cellulose. The intensity of the peaks was measured as the maximum value obtained for the peak taking into account a baseline.

2.4.7. Biodegradability of films

To study the final aerobic biodegradability of the films obtained in the present study, the methodology of the UNE-EN ISO 17556 standard was adapted as explained in Fernández-Santos et al. [19]. In summary form this assay was carried out under controlled composting conditions, in order to determine the total biodegradability of the degraded material. A constant rate of CO_2-free air entered the containers with the samples and swept along CO_2 generated. After 90 days of testing, from the datum of CO_2 produced, the biodegradability of each of the tested materials was calculated.

2.4.8. Food packing simulation

Composite films containing CNC and either CMC or CNF were used as packaging materials to seal cylindrical glass containers 4 cm in diameter holding self-produced olives. The olives were of standard size and used 24 h after harvesting (i.e., they were optimally ripe). Each container was used to place an unripe (green) olive and a ripe (brown) olive, and sealed with one of the films with the aid of paraffin at 90 °C. Tests were performed at a controlled temperature (23 °C) and relative humidity (50%) for 10 days, time during which the olives exhibited some changes. All tests were done against other materials including filter paper, plastic film, aluminum foil and a blank (no film). The specific films tested were made from CNC, CMC, CNF, CNC + CMC and CNC + CNF.

3. Results and discussion

The results were consistent with the proportions of CMC or CNF added to CNC, namely: 0% CMC (or CNF) + 100% CNC; 20% CMC/CNF + 80% CNC; 40% CMC/CNF + 60% CNC, and so forth.

3.1. Degree of substitution (DS) and mass gain in CMC

The degree of substitution in CMC was determined against cotton linters DS = 0.56 ± 0.0067, which is very similar to previously reported values for various sources of plant fiber including seaweed (0.51; [5]), grapefruit peel (0.54; [37]) and sugarcane (0.43; [38]). Naves & Petri [39] used CMC with DS = 0.7 commercially available from Aldrich; Zhang et al. [40] reported DS values of 0.23, 0.46 and 0.58; and Wahyuni et al. [41] found DS in commercial microcrystalline cellulose to range from 0.57 to 0.90 depending on the NaOH concentration and solvent used. Robles Barros et al. [42] found bleached pulp from soybean husk to have DS values of 0.95–1.56, and Zhang et al. [40] reported DS values of 0.23, 0.46 and 0.58 for laboratory-made CMC.

The degree of substitution (DS) of CMC strongly influences its solubility in water (water affinity increases with increasing DS). Thus, a polymer with DS lower than about 0.4 is insoluble, whereas one with DS > 0.4 is readily soluble in water [43]. Our polymers had DS = 0.56, so they should be water-soluble and hence suitable for various industrial uses in combination with CNC.

3.2. Morphological, optical and mechanical characterization of CNC–CMC and CNC–CNF films

3.2.1. Morphological analysis

The effect of mixing CNC with CMC or CNF on film morphology and structure was examined by scanning electron microscopy (SEM) of film cross-sections. As can be seen in Fig. 1, CNC–CNF (Fig. 1c) and CNC–CMC films (Fig. 1e) exhibited a uniform, compact appearance similar to those reported by other authors [44,45]. As can also be seen, CNF-containing films (Fig. 1b) were slightly less compact than CNC films (Fig. 1a), but CNC–CNF composite films (Fig. 1c) were quite compact as a result of the combined crystallinity of CNC and fibrillary structure of CNF. According to Kumar et al. [22], CNC gives more compact structures than does CNF by virtue of the former forming whiskers and the latter an entangled pore network [46,47]. As can be seen in Fig. 1e, CNC–CMC films were well-formed and uniform in appearance; also, they showed no signs of microscales in the matrix—which, as previously reported by other authors [48] suggests that CNC and CMC were compatible as film components.

3.2.2. FTIR and XRD analysis

Structural changes in CNC–CNF and CNC–CMC composite films were studied from their FTIR and XRD spectra, which are shown in Figs. 2, 3 and S2 —the latter in Supplementary data. The bands in the wavenumber region 3700–3000 cm^{-1} of the FTIR spectra (Fig. 2) were assigned to stretching vibrations in hydroxyl groups [49], which are affected by hydrogen bonding, and those at 2906 and 2890 cm^{-1} to aliphatic C—H bond stretching in alkyl groups [49]. The absorbance peak at 1640 cm^{-1} was assigned to H—O—H bending vibrations in adsorbed water, and the peak at ca. 1050 cm^{-1} to stretching vibrations of C—O—C bonds in pyranose rings of primary and secondary hydroxyl groups in cellulose [50]. The peak at ca. 895 cm^{-1} was due to glycoside bonds in cellulose, and those in the region 800–650 cm^{-1} were assigned to O—H vibrations [51].

Figs. 2a and S2a show the FTIR spectra for different CNC–CNF composites. As can be seen, all except that for the pure (100%) CNC film—which exhibited an additional peak at 1390 cm^{-1} due to SO_3^- ions denoted by an arrow in Fig. 2a—were identical. This result suggests that, as previously found by other authors [7], mixing CNC with CNF did not alter the chemical structure of the former. Figs. 2b and S2b show the FTIR spectra for different CNC–CMC composites. The prominent peak at 1585 cm^{-1} can be assigned to stretching in C═O bonds, and the also prominent ones at 1416 and 1314 cm^{-1} to symmetric stretching in NaCOO groups. As can be seen from Fig. S2b, the previous peaks increased with increasing proportion of CMC.

Fig. 3 shows the XRD patterns for CNC–CMC and CNC–CNF films, which were used to elucidate their crystal structure. The main diffraction angles at the 2θ values 14° (1−10), 16° (110) and 22° (200) correspond to primary diffraction in the (1–10), (110) and (200) planes, respectively, of polymorph cellulose I [52]. As can be seen in Fig. 3, the XRD spectrum for the pure CMC film contained a broad diffraction band at a 2θ value of 18–26.5° due to the amorphous nature of the polymer [53,54]. CNC–CMC composites exhibited a distinct peak for CNC at 2θ = 22.5° that was especially strong for pure CNC. Similar results were obtained by Li et al. [53] with CMC films containing CNC. Therefore, the crystal structure of CNC is not altered by the addition of CMC or CNC—the decreased crystallinity of the composites was a result of the presence of CMC or CNF. This assumption was confirmed by determining the crystallinity index (CI) of the films as calculated from Eq. (5) [36]. As can be seen from Table S1, CI was highest in CNC films

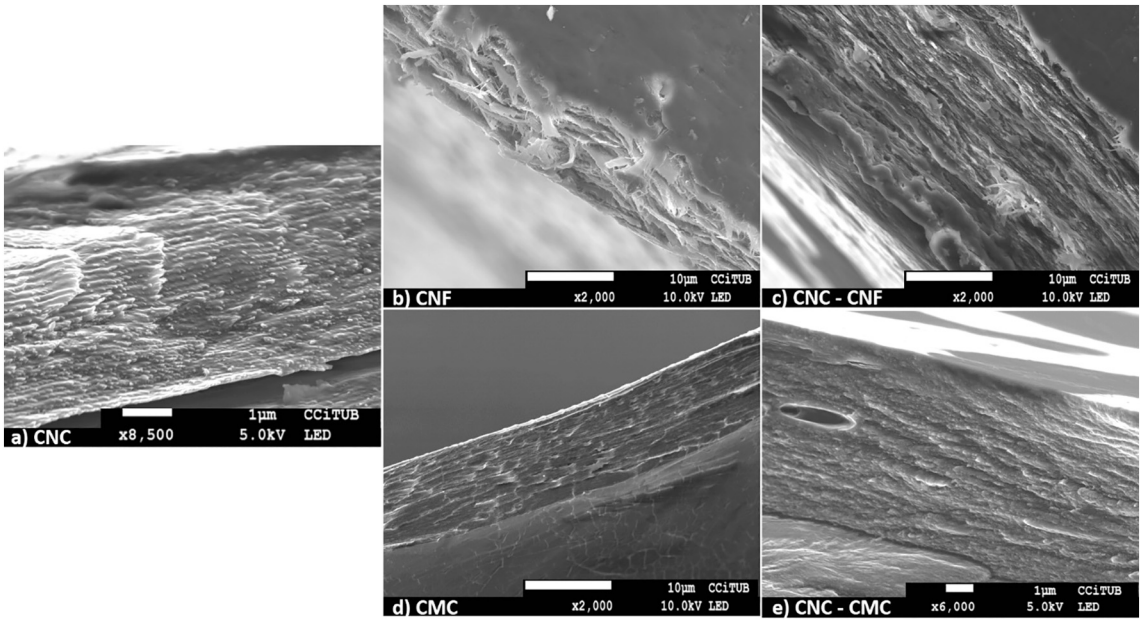

Fig. 1. Scanning electron micrographs of CNC (a), CNF (b), CNC–CNF (50–50%) (c), CMC (d), CNC–CMC (50–50%) films (e).

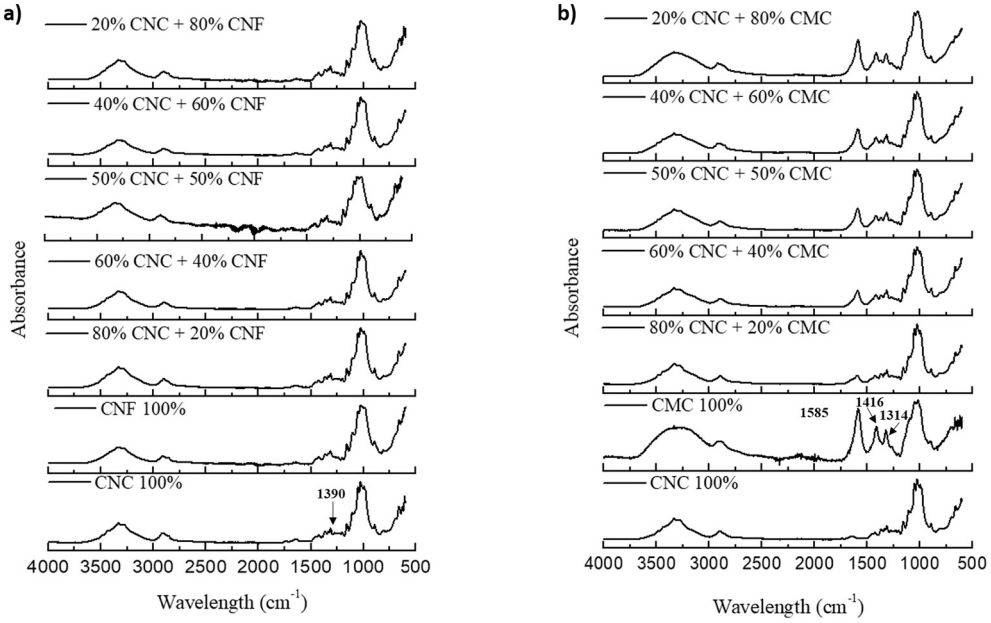

Fig. 2. FTIR spectra for CNC–CNF (a) and CNC–CMC films (b).

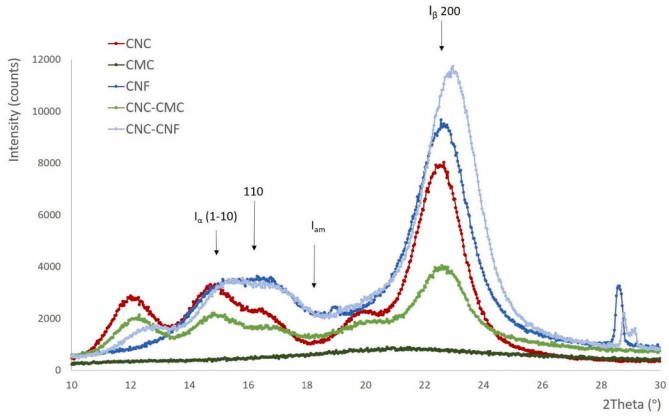

Fig. 3. XRD patterns for CNC, CMC, CNF, CNC–CMC and CNC–CNF films.

(86.64%), somewhat lower in CNF films (78.01%) and much lower in CMC films (32.94%). Also, CI for CNC–CNF and CNC–CMC composites was 82.90% and 67.73%, respectively, which is consistent with the values for the pure films.

Brinchi et al. [55] previously reported CI values of 54–88% for CNC films, and Oun & Rhim [30] found films made from rice straw, wheat straw and barley straw to have a CI value of 66.3, 71.0 and 63.4%, respectively. Xia et al. [56] reported CI = 68.5% for a CNF film and Wu et al. [57] CI = 56.3% for another made from coconut coir. Finally, Claro et al. [45] reported CI values of 90 and 85.9% for CNC films made from curaua and eucalyptus fiber, respectively, and 83.8 and 73.6% for CNF films obtained from the same materials.

The increased crystallinity of CNC films can be ascribed to suppression of amorphous regions and changes in crystal structure during production process of CNC [30]. Thus, CNC films were the least crystalline as a result of the amorphous nature of the polymer by effect of a chemical change in cellulose leading to the disappearance of the diffraction peaks at $2\theta = 16^\circ$ and $2\theta = 22^\circ$, and the appearance of the above-mentioned broad band in the 2θ region 18–26.5°. Robles Barros et al. [42] reported CI values of 21.9, 30.3 and 36.9% for CMC films obtained made from soybean husk, and unbleached pulp and bleached pulp obtained from it, respectively.

3.2.3. Optical properties

Many food packages are required to be transparent. In fact, transparent packaging allows one to check for food freshness and quality, and customers are thus more prone to buy a product if they can see through its container. In addition, transparent films allow one to see how miscible any mixed products they contain actually are.

Fig. 4 shows the transparency of CNC films containing variable proportions of CMC or CNF. As can be seen, pure CNC and CMC were both highly transparent, with a CI value of 56.08% and 77.85%, respectively. However, adding CMC to CNC decreased CI below the level for pure CNC, possibly as a result of CNC–CMC composites not being completely homogeneous. In fact, Fig. 1e) shows a zone suggestive of an air bubble.

Pure CNF films were much less transparent than pure CNC and CMC films. As a result, increasing the proportion of CNF added to CNC decreased its transparency. This result is consistent with those obtained elsewhere by mixing CNF with CNC [45] or CMC [30].

Films were also assessed for their ability to protect food from UV light. In fact, UV light passing through a package can lead to the formation of free radicals inside and result in food deterioration through fat oxidation, antioxidant decomposition, vitamin and protein denaturation, color changes or even off-odors [58]. The more strongly a film absorbs light in the 250–400 nm wavelength region, the more efficiently it will protect food from UV light. As can be seen from Fig. S3a, CNC–CMC composite films were more protective than pure CNC films; also, protective efficiency peaked in the 50%/50% composite. Absorption in the previous spectral region increased much more markedly by effect of adding CNF (Fig. S3b). Therefore, adding CMC and, especially, CNF boosted the ability of CNC to block UV light and that to prevent photochemical reactions in food as a result [59].

3.2.4. Mechanical properties

The industrial usefulness of CNC films is severely limited by their brittleness and difficult handling. However, the CNC keeps the transparency we want for our final films. Combining CNC with CNF or CMC may help to make films more flexible and less brittle while preventing breakage during handling. Film plasticity is mainly governed by mechanical properties such as tensile strength (TS) and elongation (Ɛ) [60]. The effect of adding CMC or CNF on the mechanical properties of CNC films was assessed by characterizing them in terms of TS, Ɛ and Young's

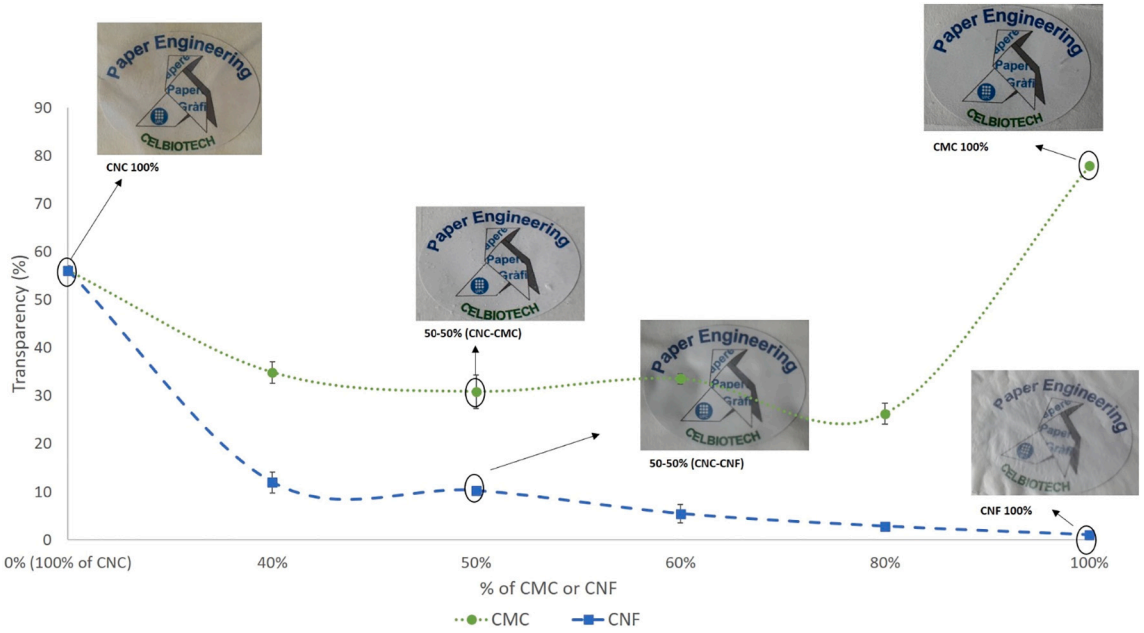

Fig. 4. Transparency of mixed films obtained by adding CMC or CNF in variable proportions to CNC.

modulus (*E*). As can be seen from Fig. 5a, increasing the proportion of CMC or CNF in the composite increased Ɛ from 0.5% for the pure CNC film to 4.07% for the pure CMC film to 8.25% for the pure CNF film. Pure CNF film exhibited the greatest elongation (up to 94% greater than that of CNC). As previously found by Djafari Petroudy [61], the lower was the crystallinity of the film material the greater was elongation. Also, elongation was smallest in the films made from CNC, which was the most crystalline polymer.

Tensile strength was 15.05 ± 0.81 MPa for pure CNC and increased with increasing proportion of CNF added (Fig. 5b). The greatest TS value for the composite films, 72.33 ± 4.35 MPa, was nearly 5 times greater than that for the film containing no CNF and that made from 40% CNF and 60% CNC. Therefore, it was the presence of CNF that increased tensile strength in the films. These results contradict the finding of Claro et al. [45] that CNC films had a greater tensile strength than CNF films. Although CMC based films were similar in tensile strength to CNF-containing films, the peak TS value for the former (48.43 ± 8.24 MPa with a CMC proportion of 40%) was lower than that for the latter.

There were no substantial differences in Young's modulus (*E*) among CNC–CNF composites. However, as can be seen from Fig. 5c, *E* decreased with increasing proportion of CMC (to 7.77 GPa in the pure CMC film). Li et al. [48] also found *E* to increase with increasing proportion of CNC; however, their pure CMC films had much smaller *E* values and greater Ɛ values than ours. These differences in mechanical properties can be ascribed to differences in the molecular weight and degree of substitution in CMC, as well as to the TS measurement conditions. In fact, the mechanical properties of CMC films were related to their degree of substitution (DS) by Chen et al. [62], who compiled the results of several studies and reported a peak tensile strength of 19 MPa for CMC films with DS values of 0.17–0.24, and one of 140.77 MPa for films of the same material and DS over the range 0.56–0.87. Our results for pure CMC films are consistent with previously reported values for similar films; thus, we measured TS = 61.49 MPa in a CMC film of DS = 0.56.

3.3. Barrier properties of CNC–CMC and CNC–CNF films

The materials typically used to pack food are polymeric petroleum derivatives with some industrial advantages such as economy, ease of handling and water-resistance; however, they are nonbiodegradable and can thus pose serious environmental hazards that are increasingly leading the food packaging industry to find more sustainable alternatives exploiting the excellent barrier properties of nanocellulose films [63].

3.3.1. Air permeance

Air permeance (AP) is one of the barrier properties most markedly influencing the performance of films for packaging. In fact, a food packaging material with a low air permeance can extend the shelf life of

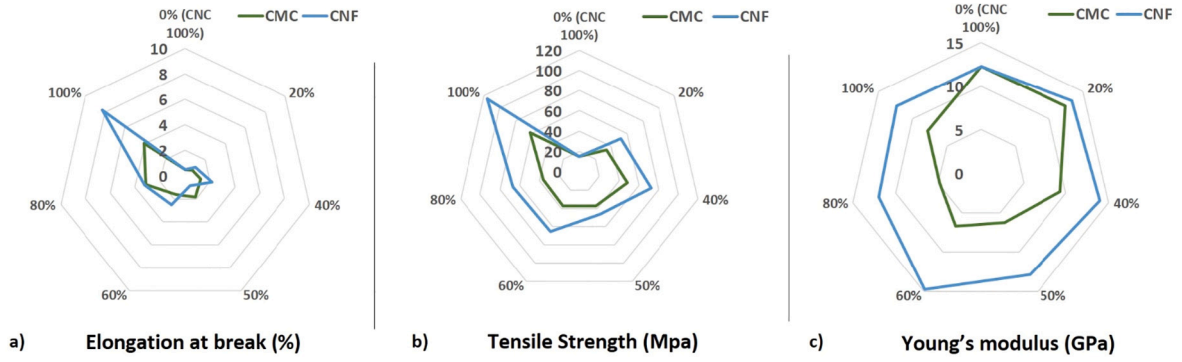

Fig. 5. Elongation at break, Tensile strength and Young's modulus of CNC–CMC and CNC–CNF films.

food. As can be seen from Table S2 (in Supplementary data), all of our films were much less air-permeant than are wood fibers and similarly permeant to bacterial cellulose [64]. Although pure CNC had AP = 2.48 ± 0.14 μm Pa^{-1} s^{-1}, pure CMC and CNF had even lower values (1.82 ± 0.02 μm and 2.18 ± 0.0 μm Pa^{-1} s^{-1}, respectively). Adding a proportion of 20–60% of CMC decreased AP in CNC but only slightly —the effect was only substantial above 80% CMC, with 2.20 ± 0.0 μm Pa^{-1} s^{-1}. Li et al. [53] found coating paper with CMC to decrease its permeance and ascribed the effect to the resistance of the polymer to penetration of gases. In this work, adding CNF to CNC considerably decreased air permeance above a CNF proportion of 60%, to a level similar to that of a composite containing 80% CNC. Our results contradict those of other authors who found CNF-containing films to have a more open structure than pure CNC films.

3.3.2. Oil resistance

Oil resistance is one other major property of films to be used for packaging. All CNC–CMC and CNC–CNF films studied here were oil-resistant (see Fig. S4 of supplementary data). In fact, there were no signs of oil crossing them after 1800 s in all of the films.

Several authors have reported the oil resistance ability of nanocelluloses. In most cases they were used for creating a coating layer over paper or wood. For example, Gicquel et al., [65] obtained that CNC increased oil resistance of paper although in smaller amounts than other authors that used MFC [66]. On the other hand, Hossain et al. [63] coated wood flour composites with NFC. All of them obtained that oil resistance was increased after coating. They justify this effect by the reduction in the number and size of pores in the paper or wood matrix by the coating materials. They also obtained that the increased oil resistance of papers was strongly related with the reduced air permeability. Dai et al. [67] obtained multilayer films of NFC and guar gum, they proposed several theories justifying the increased oil resistance, like the compact and dense structure of film, the presence of a water layer that could prevent the oil from dissolving in the film or the impermeability against oil of the crystalline part of cellulose nanofibrils. Other works have also shown the ability of CMC in creating oil resistance in combination with other materials [68].

Therefore, since we obtained complete oil resistance films, we can state that all of our films were dense and defect-free enough to avoid oil penetration.

3.3.3. Resistance to moisture and water vapor

One of the most serious drawbacks of polysaccharide based films is their high sensitivity to moisture, which severely restricts their real-life use (especially for food packaging) [63,68]. Mixing different types of cellulose may improve their barrier properties by forming too hard and winding a network for molecules to pass through. The mixed films studied here were subjected to the water drop test (WDT) in order to determine the time they took to adsorb a drop of water, and the water contact angle (WCA) test in order to assess hydrophobicity. Also, they were used to measure resistance to water vapor, which is one of the critical properties of materials to be used for food packaging —in fact, some foods must be prevented as far as possible from exposure to moisture through their packaging [69,70].

As can be seen from Fig. 6a, the time needed to adsorb a drop of water was shorter in pure CMC films than it was in pure CNC films (20 vs 55 min). This result is consistent with the presence of carboxyl groups in CMC and its low crystallinity relative to CNC [30]. WDT decreased dramatically above a CMC content of 20% and rapidly reached the levels for pure CMC with increasing proportion of this component in the films. By contrast, CNF-containing films had virtually the same WDT values as pure CNC films.

The water contact angle (WCA-Fig. 6b) for pure CNC (44.7° ± 2.5) was similar to those for the cotton linter-based CNC films obtained by Beltramino et al. [47] and those for the CNF/CNC double-layer coating system of Tyagi et al. [7]. Pure CMC had WCA = 65.9° ± 0.25, which exceeds the values reported by Oun & Rhim [30] (41°), Ezati et al. [71] (41.9°) and Kim et al. [17] (33.9°). Also, WCA for pure CNF (79.0 ± 6.6°) was greater than the value reported by Kim et al. [17] for CNF treated with endoglucanase (45°) and also than that obtained by Ezati et al. [71] (59.3°). The water contact angle (WCA), which can be defined as the angle at which the liquid/vapor interface meets a solid substrate with water as testing fluid, is a measure of surface wettability [7].

Hydrophobicity and hydrophilicity can be affected by various factors including surface chemistry and roughness [72]. However, WDT and WCA are not always mutually related. Thus, Fernández-Santos et al. [19] found plasticizers to increase WDT in CNC films at the expense of decreasing WCA. Since all of the obtained films had a similar roughness (data not shown) the results of WCA can be compared between them. As can be seen from Fig. 6b, which contradicts the WDT results (Fig. 6a), adding CMC increased WCA in CNC. Thus, a CMC proportion of only 20% led to the same WCA level as in pure CMC. Oun & Rhim [30] also previously found WCA to decrease with increasing proportion of CNC. The presence of CNF also increased WCA, the films containing it in a proportion of 80% having angles comparable to those of pure CNF. Claro et al. [45] obtained similar results with CNC- and CNF-containing films made from curaua nanocellulose. According to Vogler [73], hydrophobic surfaces have WCA > 65°; therefore, CNC films containing at least 80% CNF can be deemed hydrophobic.

Fig. 7 shows WVTR for our films as measured at 50% and 90% relative humidity (RH). The WVTR value for pure CNC at RH = 50%, 3 g m^{-2} day^{-1}, was higher than those for pure CMC and CNF (1.20 and 1.23 g m^{-2} day^{-1}, respectively), pure CMC having the lowest values. On the other hand, Kim et al. [17] obtained low WVTR values for CNF films relative to CMC. As can be seen from Fig. 7a for CNC–CMC films and Fig. 7b for CNC–CNF films, WVTR decreased slightly with increasing proportion of CMC and CNF, respectively. Oun & Rhim [30], and Li et al. [53], found WVTR to increase with increasing proportion of CMC. On the other hand, Tyagi et al. [7] found no significant differences in WVTR

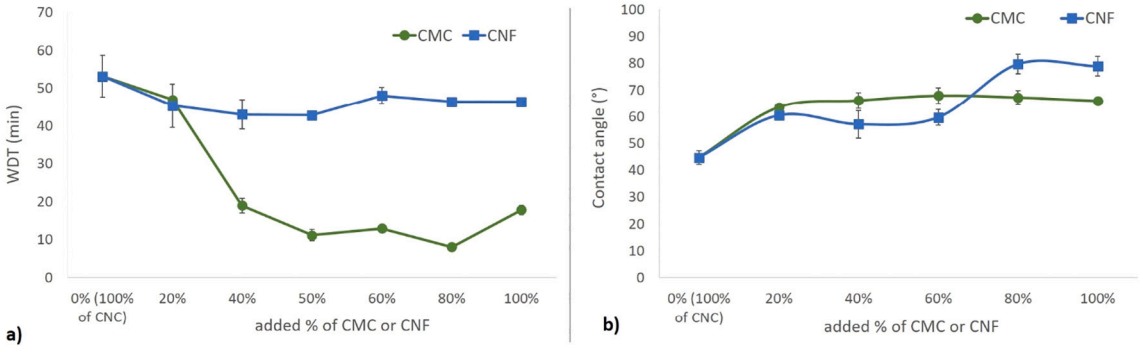

Fig. 6. a) WDT values (min) and b) Water contact angle (°) for CNC–CMC and CNC–CNF films.

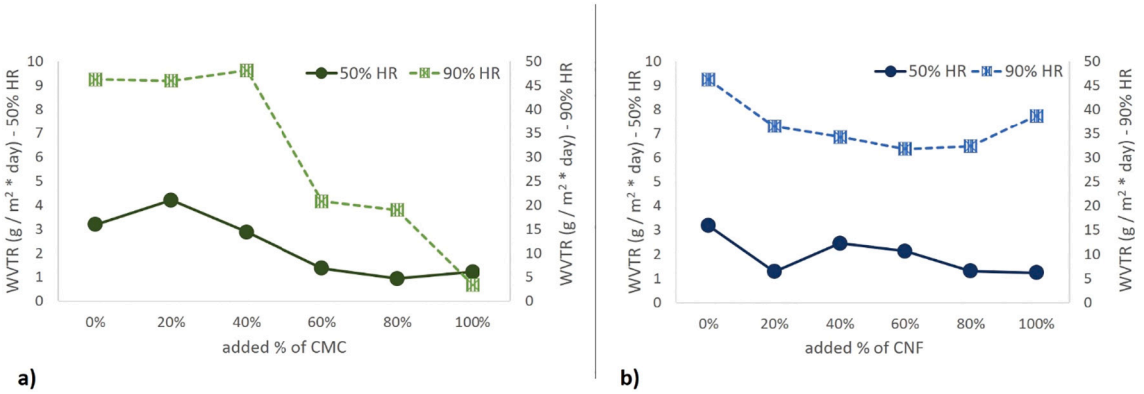

Fig. 7. Water vapor transmission rate of CNC–CNF (a) and CNC–CMC films (b).

between CNC and CNF composites used as paper coatings.

WVTR was greater at RH = 90% than it was at RH = 50%. In fact, an increased relative humidity increases saturation of water binding sites and can increase film permeability to water vapor [74]. As can be seen from Fig. 7b, an increased proportion of CNF (Fig. 7b) increased film resistance to water vapor; the effect, however, was much more marked with CMC (Fig. 7a). Thus, WVTR decreased considerably above 40% CMC and rapidly dropped to the level for pure CMC. Surprisingly, pure CMC had a very low WVTR at RH = 90% (3.38 g m^{-2} day^{-1}, which is similar to that measured at RH = 50%). The high conformability of CMC chain contributes to form dense, compact and defect-free films. He et al. [75] reported that with increasing the CMC content, the network structure become denser. This dense structure was the responsible of providing such a good resistance to water vapor in our films. As we increased the amount of CNC, this compact structure can be broken creating areas through which water vapor can go across. With increased amounts of CNC, crystals of this nanocellulose as well as its free OH groups disrupted this continuity and density in the network of CMC, this effect being more visible at high relative humidity. In fact, Jeffrey et al., 2018 [76] reported that CNC created CNC-aggregated domains that reduced barrier properties of a CMC-chitosan complex. Interestingly, no WVTR measurements of CMC films at so high moisture levels appear to have been reported to date.

3.3.4. *Oxygen permeability*

Oxygen permeability (OP) in the films was assessed under a wide range of moisture conditions here (RH values from 0 to 90%). As can be seen from Fig. 8, pure CNC lost its oxygen- impermeability above RH = 20%—in fact, no further measurements could be done because films broke above 60% RH. In previous work (Fernández-Santos et al. [19]), our group observed a similar behavior in CNC films, and the addition of a plasticizer such as xylitol, maltitol or sorbitol to extend their resistance to RH = 60%. As can be seen from Fig. 8, increasing the proportion of CMC or CNF made the films completely oxygen- impermeability up to RH = 60%. De Oliveira et al. [74] previously found the oxygen permeability of films made from soy protein isolate (SPI) to be improved by adding increasing amounts of CMC. Also, Tyagi et al. [7] found CNF to have excellent oxygen-barrier properties which, however, were considerably degraded by the presence of moisture. Because of its high crystallinity, CNC is less sensitive to moisture but also more fragile—so, as seen in our films, it tends to easily break and allow the passage of oxygen. Mixing CNC with CNF here decreased OP relative to pure CNC and CNF. Hydrogen bonding plays a central role in OP at low moisture levels as its restricts motion of CNF fibrils, thereby preventing oxygen molecules to go through the evacuated volume. Hydrogen bonds break at high moisture levels, and cause CNF fibrils to separate and swell [77]. This was probably the origin of the substantially improved oxygen permeability of our CNC- and CNF-containing films. Thus, CNC may help prevent defibrillation and hence the passage of oxygen. Virtanen et al. [78] reported an OP value of 50,000 $cm^3 \cdot \mu m/m^2 \cdot day \cdot atm$ for CNF–PVA films and one of 48,000 $cm^3 \cdot \mu m/m^2 \cdot day \cdot atm$ for epoxy-CNF–PVA films as measured at RH = 90%. We obtained similar values for pure CNF (55,597.28 $cm^3 \cdot \mu m/m^2 \cdot day \cdot atm$), but somewhat lower levels for CNC–CNF composites (21,089.28 $cm^3 \cdot \mu m/m^2 \cdot day \cdot atm$). Also, the oxygen impermeability of our CNC–CMC and CNC–CNF films at RH = 80% exceeded that of CNC films mixed with plasticizers to improve their barrier properties [19].

According to Gao et al. [79], a material with an OP value of 40–400 $cm_3 \cdot \mu m/m^2 \cdot day \cdot atm$ is highly oxygen-impermeability. Therefore, our CMC, CNF, CNC–CMC and CNC–CNF films were all resistant to the passage of oxygen below RH = 60% and are thus suitable for use as food packaging materials as they will efficiently protect their contents from the deleterious effects of oxygen.

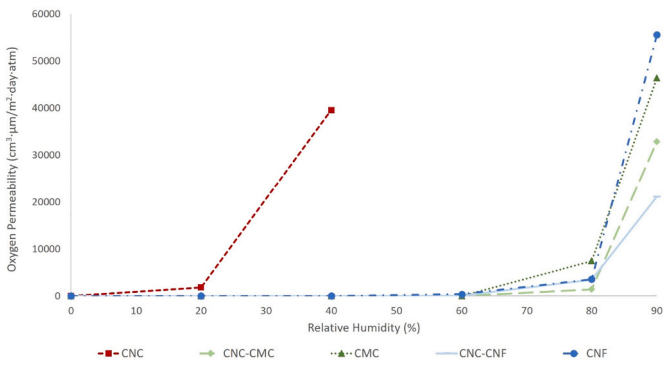

Fig. 8. Oxygen permeability (OP) of CNC–CMC (50–50%) and CNC–CNF (50–50%) films.

3.4. *Biodegradability*

Adding CNF or CMC to CNC made the resulting films suitable for various uses including food packaging. However, the films should also be biodegradable in order to retain usability. This led us to assess biodegradability in pure CNC, CMC and CNF films, and also in CNC films containing 50% CMC or CNF. As can be seen from Fig. 9, the films containing either CMC or CNF were more biodegradable than the pure films. Thus, CNC led to less marked CO_2 accumulation (i.e., there was less CO_2 forming by microbial metabolism). Fernández-Santos et al. [19] found CNC to be made more biodegradable by addition of natural plasticizers. As can be seen, mixing CNC with CMC or CNF here considerably increased its biodegradability. Thus, biodegradability after 90 days was highest in CNC–CNF composites, followed by CNC–CMC composites and then by pure CMC and CNF. Therefore, CNF was more easily degraded than was CNC, which can be ascribed to the presence of

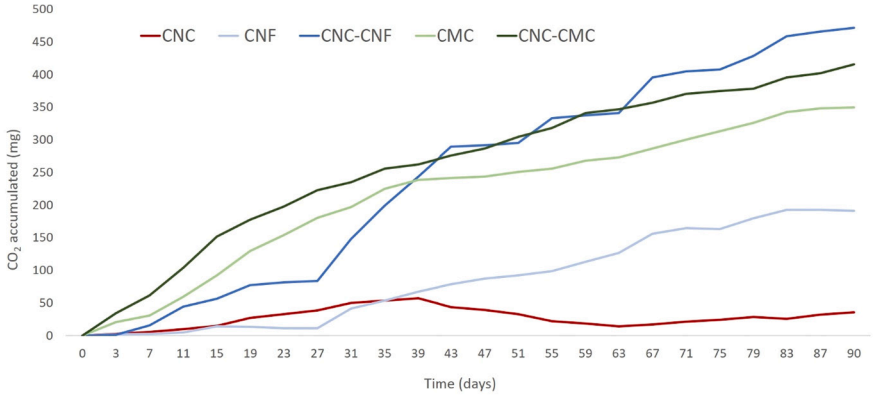

Fig. 9. Biodegradability, in terms of CO_2 accumulation, of pure CNC, CMC and CNF, and their 50–50% combinations.

amorphous regions in cellulose making CNF more accessible to microorganisms [80]. Similarly, the lower crystallinity of CMC (Table S1) probably resulted in easier access by microbes.

PLA was used as a control to evaluate if the level of biodegradability of our films was optimal compared to other materials already described as biodegradable [81]. After 30 days of testing, the accumulated CO_2 (mg) values obtained were: 49.79 for 100% CNC film, 41.21 for 100% CNF, 196.60 for 100% CMC, 148.35 for CNC–CNF, 235.03 for CNC–CMC

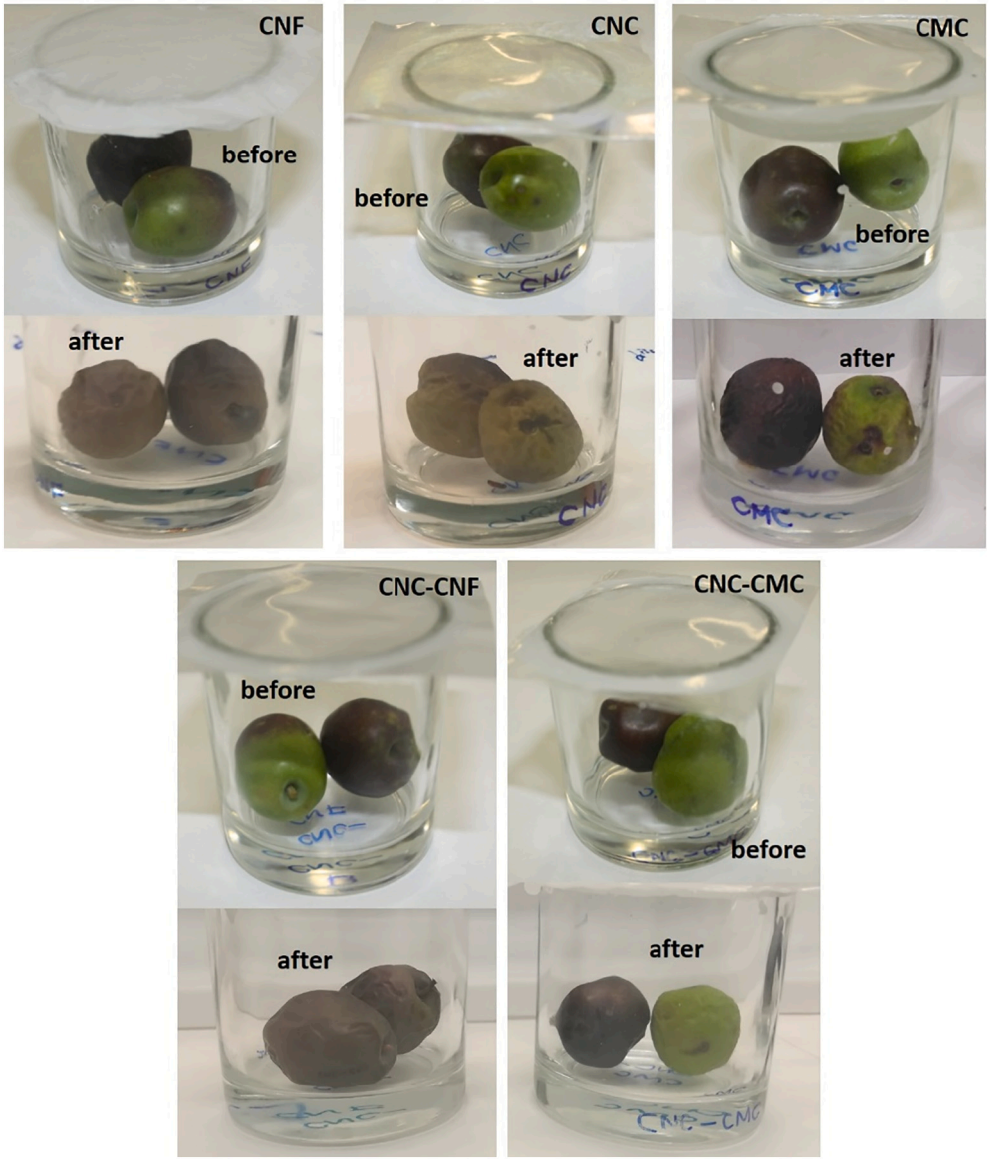

Fig. 10. Appearance of olives before and after storage under pure CNC, CNF and CMC, and their 50–50% combinations, for 10 days.

and 108.83 for PLA. Therefore, after 30 days, some of our films have already biodegraded more than PLA.

These results indicated that the biodegradability of our films was optimal. Moreover, these results support using the studied composites to replace nonbiodegradable, environmentally unfriendly plastics that can have added deleterious effects on health and the economy. No studies comparing biodegradability in different types of nanocellulose appear to have been conducted to date.

3.5. Food packaging simulation

As stated above, the addition of CMC or CNF to CNC protected the ensuing films from the passage of oxygen and water vapor, thereby probably resulting in better preservation of food. This assumption was confirmed by food packaging simulation tests. Food packaging is the critical point for the correct handling and maintenance of food quality [10]. Food quality depends on a number of factors among which shelf life is a prominent one. The shelf life of food can be diminished by the presence of oxygen, moisture and microbes, which accelerate decomposition processes [79]. The test was carried out with olives for several reasons: it is a small fruit, with a specific surface area that is easy to analyze and observe possible changes in it; it is a fruit with a short degradation period in environmental conditions once it is removed from the tree; and it is a fruit that we have our own production, so we can be sure that it has not been treated with any preservative that could falsify the results obtained. Table S3 shows the results of a simulation test where different types of film were used to store olives for 10 days. Deterioration was assessed in terms of changes in appearance (specifically, in olive hardness, color and skin smoothness). The results were compared with those provided by standard food packaging materials (paper, aluminum foil, plastic film) and a blank (no container).

As can be seen from Fig. 10 and Table S3, pure CMC and CNC–CMC composites were the materials best preserving the initial appearance of the olives—even better than standard plastic and aluminum foil (see Fig. S5). In fact, the plastic and foil containers preserved the olives well as regards color and surface smoothness, but were the only materials that contained moisture at the end of the test (Fig. S5). The absence of moisture is essential to avoid fungal growth, marked with a black arrow in the Fig. S5. The olives stored in pure CNF had a more degraded overall appearance as regards color—which turned brown with time. This was also the case with CNC–CNF composites. Therefore, CMC is to be preferred to CNF as it reduced oxygen exchange with the outside and delayed ripening—thereby extending the shelf life of the olives. These results are quite consistent with those of the oxygen permeance and WVTR tests (Table S4).

4. Conclusions

In this work, commercial CNC was mixed with commercially available CNF and laboratory-made CMC of DS = 0.56 in different proportions (0/100, 20/80, 40/60, 50/50, 60/40, 80/20 and 100/0) to obtain films with advanced properties for use as food packaging materials. As seen by scanning electron microscopy (SEM), film morphology was uniform and compact. Also, as shown by FTIR spectra, the films exhibited no adverse changes in chemical structure. In addition, the high crystallinity of pure CNC was reduced by the presence of CNF and, especially, CMC.

The most relevant properties of the films for use as packaging materials were found to change with the proportion of CMC or CNF added to CNC. Thus, CMC-containing films were the most transparent and CNF-containing films the least. Both CMC and CNF increased protection from UV light, which is especially useful when storing food. As regards mechanical properties, 100% CNF film increased elongation (by up to 95%) relative to pure CNC, and so did CMC, albeit to a less marked extent. CNF-containing films were also those exhibiting the greatest tensile strength (TS), which peaked in those with a 40% proportion. CMC also increased TS, but less markedly.

CNF (more significantly from 60%) and CMC (more significantly from 80%) both decreased air permeability and all, pure and composite films, were fully oil-resistant. Composite films, but especially those containing CNF (especially at 80%), were more hydrophobic than pure films; concerning the mixtures with CMC, the effect was noticeable at 40%. The WVTR test provided interesting results. Thus, under high moisture conditions (RH = 90%), the presence of CNF or, especially, CMC, increased the water vapor resistance of the films. Below a relative humidity of 60%, all types of films were highly resistant to oxygen and hence protective from its deleterious effects. The environmental suitability of the composite films as replacements for existing plastic materials is further supported by the results of biodegradability tests run for 90 days. Finally, the films performed quite well as packaging materials for olives stored under ambient conditions. Pure CMC and CNC–CMC composites excelled in this respect as they preserved olive quality for 10 days and could therefore be used to extend their shelf life. Overall, CNC–CMC and CNC–CNF composites have a promising potential as food packaging materials.

Acknowledgements

This publication is part of the PID2020-114070RB-I00 (CELLECO-PROD) project, funded by MCIN/AEI/10.13039/501100011033. The authors would also like to thank the consolidated research group AGAUR 2017 SGR 30 with Universitat de Barcelona (UB) and to the Serra Húnter Fellowship awarded to O. Cusola. With the support from the Secretariat for Universities and Research of the Ministry of Business and Knowledge of the Government of Catalonia and the European Social Fund.

Appendix A. Supplementary data

Supplementary data to this article can be found online at https://doi.org/10.1016/j.ijbiomac.2022.05.049.

References

[1] J. Wróblewska-Krepsztul, T. Rydzkowski, G. Borowski, M. Szczypiński, T. Klepka, V.K. Thakur, Recent progress in biodegradable polymers and nanocomposite-based packaging materials for sustainable environment, Int. J. Polym. Anal. Charact. 23 (4) (2018) 383–395.
[2] J.F. Rubilar, D. Candia, A. Cobos, O. Díaz, F. Pedreschi, Effect of nanoclay and ethyl-Nα-dodecanoyl-l-arginate hydrochloride (LAE) on physico-mechanical properties of chitosan films, LWT - Food Sci Technol. 72 (2016) 206–214, https://doi.org/10.1016/j.lwt.2016.04.057.
[3] N. Chausali, J. Saxena, R. Prasad, Recent trends in nanotechnology applications of bio-based packaging, J. Agric. Food Res. 7 (2022), 100257, https://doi.org/10.1016/j.jafr.2021.100257.
[4] R. Tharanathan, Biodegradable films and composite coatings: past, present and future, Trends Food Sci. Technol. 14 (3) (2003) 71–78. https://linkinghub.elsevier.com/retrieve/pii/S0924224402002807.
[5] D.S. Lakshmi, N. Trivedi, C.R.K. Reddy, Synthesis and characterization of seaweed cellulose derived carboxymethyl cellulose, Carbohydr. Polym. 157 (2017) 1604–1610. https://linkinghub.elsevier.com/retrieve/pii/S0144861716313078.
[6] E. Quintana, M. Ago, C. Valls, M.B. Roncero, O.J. Rojas, Alternative chemo-enzymatic treatment for homogeneous and heterogeneous acetylation of wood fibers, Cellulose 25 (9) (2018) 5323–5336, https://doi.org/10.1007/s10570-018-1947-4.
[7] P. Tyagi, L.A. Lucia, M.A. Hubbe, L. Pal, Nanocellulose-based multilayer barrier coatings for gas, oil, and grease resistance, Carbohydr. Polym. 206 (October 2018) (2019) 281–288, https://doi.org/10.1016/j.carbpol.2018.10.114.
[8] H. Kono, Characterization and properties of carboxymethyl cellulose hydrogels crosslinked by polyethylene glycol, Carbohydr. Polym. 106 (1) (2014) 84–93, https://doi.org/10.1016/j.carbpol.2014.02.020.
[9] N. Lavoine, I. Desloges, J. Bras, Microfibrillated cellulose coatings as new release systems for active packaging, Carbohydr. Polym. 103 (1) (2014) 528–537, https://doi.org/10.1016/j.carbpol.2013.12.035.
[10] A. Ashfaq, N. Khursheed, S. Fatima, Z. Anjum, K. Younis, Application of nanotechnology in food packaging: pros and cons, J. Agric. Food Res. 7 (January) (2022), 100270, https://doi.org/10.1016/j.jafr.2022.100270.
[11] M.A. Hubbe, A. Ferrer, P. Tyagi, Y. Yin, C. Salas, L. Pal, et al., Nanocellulose in thin films, coatings, and plies for packaging applications: a review, BioResources 12 (1)

(2017) 2143–2233. http://ojs.cnr.ncsu.edu/index.php/BioRes/article/view/11063.
[12] E. Csiszár, S. Nagy, A comparative study on cellulose nanocrystals extracted from bleached cotton and flax and used for casting films with glycerol and sorbitol plasticisers, Carbohydr. Polym. 174 (2017) 740–749, https://doi.org/10.1016/j.carbpol.2017.06.103.
[13] F. Beltramino, M. Blanca Roncero, T. Vidal, C. Valls, A novel enzymatic approach to nanocrystalline cellulose preparation, Carbohydr. Polym. 189 (February) (2018) 39–47.
[14] N. Grishkewich, N. Mohammed, J. Tang, K.C. Tam, Recent advances in the application of cellulose nanocrystals, Curr. Opin. Colloid Interface Sci. 29 (2017) 32–45, https://doi.org/10.1016/j.cocis.2017.01.005.
[15] J. Tang, J. Sisler, N. Grishkewich, K.C. Tam, Functionalization of cellulose nanocrystals for advanced applications, J. Colloid Interface Sci. 494 (2017) 397–409, https://doi.org/10.1016/j.jcis.2017.01.077.
[16] N. Johar, I. Ahmad, A. Dufresne, Extraction, preparation and characterization of cellulose fibres and nanocrystals from rice husk, Ind. Crops Prod. 37 (1) (2012) 93–99.
[17] H.-J. Kim, S. Roy, J.-W. Rhim, Effects of various types of cellulose nanofibers on the physical properties of the CNF-based films, J. Environ. Chem. Eng. 9 (5) (2021), 106043, https://doi.org/10.1016/j.jece.2021.106043.
[18] S. Belbekhouche, J. Bras, G. Siqueira, C. Chappey, L. Lebrun, B. Khelifi, et al., Water sorption behavior and gas barrier properties of cellulose whiskers and microfibrils films, Carbohydr Polym. 83 (4) (2011) 1740–1748.
[19] J. Fernández-Santos, C. Valls, O. Cusola, M.B. Roncero, Improving filmogenic and barrier properties of nanocellulose films by addition of biodegradable plasticizers, ACS Sustain. Chem. Eng. 9 (29) (2021) 9647–9660. https://pubs.acs.org/doi/10.1021/acssuschemeng.0c09109.
[20] L. Zhang, J. Zhao, Y. Zhang, F. Li, X. Jiao, Q. Li, The effects of cellulose nanocrystal and cellulose nanofiber on the properties of pumpkin starch-based composite films, Int. J. Biol. Macromol. 192 (17) (2021) 444–451, https://doi.org/10.1016/j.ijbiomac.2021.09.187.
[21] N.A. El-wakil, E.A. Hassan, R.E. Abou-zeid, A. Dufresne, Development of wheat gluten / nanocellulose / titanium dioxide nanocomposites for active food packaging, Carbohydr. Polym. 124 (2015) 337–346, https://doi.org/10.1016/j.carbpol.2015.01.076.
[22] V. Kumar, R. Bollström, A. Yang, Q. Chen, G. Chen, P. Salminen, et al., Comparison of nano- and microfibrillated cellulose films, Cellulose 21 (5) (2014) 3443–3456, https://doi.org/10.1007/s10570-014-0357-5.
[23] D. Trache, M.H. Hussin, M.K.M. Haafiz, V.K. Thakur, Recent progress in cellulose nanocrystals: sources and production, Nanoscale 9 (5) (2017) 1763–1786. http://xlink.rsc.org/?DOI=C6NR09494E.
[24] P. Rezayati Charani, M. Dehghani-Firouzabadi, E. Afra, A. Shakeri, Rheological characterization of high concentrated MFC gel from kenaf unbleached pulp, Cellulose 20 (2) (2013) 727–740. http://link.springer.com/10.1007/s10570-013-9862-1.
[25] T. Heinze, K. Pfeiffer, Studies on the synthesis and characterization of carboxymethylcellulose, Die Angew. Makromol. Chem. 266 (1) (1999) 37–45. http://doi.wiley.com/10.1002/%28SICI%291522-9505%2819990501%29266%3A1%3C37%3A%3AAID-APMC37%3E3.3.CO%3B2-Q.
[26] R. Priyadarshi, B. Kumar, J.W. Rhim, Green and facile synthesis of carboxymethylcellulose/ZnO nanocomposite hydrogels crosslinked with Zn2+ ions, Int. J. Biol. Macromol. 162 (2020) 229–235, https://doi.org/10.1016/j.ijbiomac.2020.06.155.
[27] A.A. Oun, J.W. Rhim, Characterization of carboxymethyl cellulose-based nanocomposite films reinforced with oxidized nanocellulose isolated using ammonium persulfate method, Carbohydr. Polym. 174 (2017) 484–492.
[28] S. Roy, J.W. Rhim, Carboxymethyl cellulose-based antioxidant and antimicrobial active packaging film incorporated with curcumin and zinc oxide, Int. J. Biol. Macromol. 148 (2020) 666–676.
[29] K.M. Tavares, A. de Campos, B.R. Luchesi, A.A. Resende, J.E. de Oliveira, J. M. Marconcini, Effect of carboxymethyl cellulose concentration on mechanical and water vapor barrier properties of corn starch films, Carbohydr. Polym. 246 (February) (2020), 116521, https://doi.org/10.1016/j.carbpol.2020.116521.
[30] A.A. Oun, J.-W. Rhim, Isolation of cellulose nanocrystals from grain straws and their use for the preparation of carboxymethyl cellulose-based nanocomposite films, Carbohydr. Polym. 150 (2016) 187–200. https://linkinghub.elsevier.com/retrieve/pii/S0144861716305331.
[31] A.A. Oun, J.-W. Rhim, Preparation and characterization of sodium carboxymethyl cellulose/cotton linter cellulose nanofibril composite films, Carbohydr. Polym. 127 (2015) 101–109, https://doi.org/10.1016/j.carbpol.2015.03.073.
[32] B.L. Browning, in: Carboxymehylcellulose. Methods of Wood Chemistry Vol. II, Interscience, New York/London/Sydney, 1967, pp. 490–491.
[33] ASTM Methods, D1439-61T. Tentative Methods of Testing Sodium Carboxymethyl Cellulose, 1961.
[34] H. Togrul, Production of carboxymethyl cellulose from sugar beet pulp cellulose and rheological behaviour of carboxymethyl cellulose, Carbohydr Polym. 54 (1) (2003) 73–82. https://linkinghub.elsevier.com/retrieve/pii/S0144861703001474.
[35] J.H. Han, J.D. Floros, Casting antimicrobial packaging films and measuring their physical properties and antimicrobial activity, J. Plast Film Sheeting 13 (4) (1997) 287–298.
[36] L. Segal, J.J. Creely, A.E. Martin, C.M. Conrad, An empirical method for estimating the degree of crystallinity of native cellulose using the X-ray diffractometer, Text Res J. 29 (10) (1959) 786–794, https://doi.org/10.1177/004051755902901003.
[37] J. Chumee, DS, Cellulose extraction from pomelo peel: synthesis of carboxymethyl cellulose, Int. J. Mater. Metall. Eng. 8 (8) (2014) 435–437. https://waset.org/publications/9998337/cellulose-extraction-from-pomelo-peel-synthesis-of-carboxymethyl-cellulose.
[38] K.M. Hong, Preparation and Characterization of Carboxymethyls Cellulose From Sugarcane Bagasse, Malaysia Tunku Abdul Rahman Univ., 2013.
[39] A.F. Naves, D.F.S. Petri, The effect of molecular weight and degree of substitution on the interactions between carboxymethyl cellulose and cetyltrimethylammonium bromide, Colloids Surf. A Physicochem. Eng. Asp. 254 (1–3) (2005) 207–214. https://linkinghub.elsevier.com/retrieve/pii/S0927775704009239.
[40] C. Zhang, X. Yang, Y. Li, C. Qiao, S. Wang, X. Wang, et al., Enhancement of a zwitterionic chitosan derivative on mechanical properties and antibacterial activity of carboxymethyl cellulose-based films, Int. J. Biol. Macromol. 159 (2020) 1197–1205, https://doi.org/10.1016/j.ijbiomac.2020.05.080.
[41] H.S. Wahyuni, S. Yuliasmi, H.S. Aisyah, D. Riati, Characterization of synthesized sodium carboxymethyl cellulose with variation of solvent mixture and alkali concentration, Open Access Maced. J. Med. Sci. 7 (22) (2019) 3878–3881. https://spiroski.migration.publicknowledgeproject.org/index.php/mjms/article/view/oamjms.2019.524.
[42] P.J. Robles Barros, D.P. Ramirez Ascheri, M.L. Siqueira Santos, C.C. Morais, J. L. Ramirez Ascheri, R. Signini, et al., Soybean hulls: optimization of the pulping and bleaching processes and carboxymethyl cellulose synthesis, Int. J. Biol. Macromol. 144 (2020) 208–218, https://doi.org/10.1016/j.ijbiomac.2019.12.074.
[43] M.J. Waring, D. Parsons, Physico-chemical characterisation of carboxymethylated spun cellulose fibres, Biomaterials 22 (9) (2001) 903–912. http://www.ncbi.nlm.nih.gov/pubmed/11311009.
[44] M.-C. Li, C. Mei, X. Xu, S. Lee, Q. Wu, Cationic surface modification of cellulose nanocrystals: toward tailoring dispersion and interface in carboxymethyl cellulose films, Polymer (Guildf). 107 (2016) 200–210, https://doi.org/10.1016/j.polymer.2016.11.022.
[45] P. Claro, A. de Campos, A. Corrêa, V. Rodrigues, B. Luchesi, L. Silva, et al., Curaua and eucalyptus nanofiber films by continuous casting: mixture of cellulose nanocrystals and nanofibrils, Cellulose 26 (4) (2019) 2453–2470, https://doi.org/10.1007/s10570-019-02280-9.
[46] R. Bardet, C. Reverdy, N. Belgacem, I. Leirset, K. Syverud, M. Bardet, et al., Substitution of nanoclay in high gas barrier films of cellulose nanofibrils with cellulose nanocrystals and thermal treatment, Cellulose 22 (2) (2015) 1227–1241, https://doi.org/10.1007/s10570-015-0547-9.
[47] F. Beltramino, M.B. Roncero, T. Vidal, A.L. Torres, C. Valls, Increasing yield of nanocrystalline cellulose preparation process by a cellulase pretreatment, Bioresour. Technol. 192 (2015) 574–581, https://doi.org/10.1016/j.biortech.2015.06.007.
[48] M.-C. Li, C. Mei, X. Xu, S. Lee, Q. Wu, Cationic surface modification of cellulose nanocrystals: toward tailoring dispersion and interface in carboxymethyl cellulose films, Polymer (Guildf) 107 (2016) 200–210. https://linkinghub.elsevier.com/retrieve/pii/S0032386116310151.
[49] P. Cazón, M. Vázquez, G. Velazquez, Cellulose-glycerol-polyvinyl alcohol composite films for food packaging: evaluation of water adsorption, mechanical properties, light-barrier properties and transparency, Carbohydr Polym. 195 (January) (2018) 432–443, https://doi.org/10.1016/j.carbpol.2018.04.120.
[50] M. Rouhi, S.H. Razavi, S.M. Mousavi, Optimization of crosslinked poly(vinyl alcohol) nanocomposite films for mechanical properties, Mater Sci Eng C. 71 (2017) 1052–1063, https://doi.org/10.1016/j.msec.2016.11.135.
[51] M. Mujtaba, A.M. Salaberria, M.A. Andres, M. Kaya, A. Gunyakti, J. Labidi, Utilization of flax (Linum usitatissimum) cellulose nanocrystals as reinforcing material for chitosan films, Int. J. Biol. Macromol. 104 (2017) 944–952, https://doi.org/10.1016/j.ijbiomac.2017.06.127.
[52] R.J. Moon, A. Martini, J. Nairn, J. Simonsen, J. Youngblood, Cellulose nanomaterials review: structure, properties and nanocomposites, Chem Soc Rev. 40 (7) (2011) 3941. http://xlink.rsc.org/?DOI=c0cs00108b.
[53] H. Li, H. Shi, Y. He, X. Fei, L. Peng, Preparation and characterization of carboxymethyl cellulose-based composite films reinforced by cellulose nanocrystals derived from pea hull waste for food packaging applications, Int. J. Biol. Macromol. 164 (2020) 4104–4112, https://doi.org/10.1016/j.ijbiomac.2020.09.010.
[54] N. Jannatyha, S. Shojaee-Aliabadi, M. Moslehishad, E. Moradi, Comparing mechanical, barrier and antimicrobial properties of nanocellulose/CMC and nanochitosan/CMC composite films, Int. J. Biol. Macromol. 164 (2020) 2323–2328, https://doi.org/10.1016/j.ijbiomac.2020.07.249.
[55] L. Brinchi, F. Cotana, E. Fortunati, J.M. Kenny, Production of nanocrystalline cellulose from lignocellulosic biomass: technology and applications, Carbohydr Polym. 94 (1) (2013) 154–169, https://doi.org/10.1016/j.carbpol.2013.01.033.
[56] J. Xia, Z. Zhang, W. Liu, V.C.F. Li, Y. Cao, W. Zhang, et al., Highly transparent 100% cellulose nanofibril films with extremely high oxygen barriers in high relative humidity, Cellulose 25 (7) (2018) 4057–4066, https://doi.org/10.1007/s10570-018-1843-y.
[57] J. Wu, X. Du, Z. Yin, S. Xu, S. Xu, Y. Zhang, Preparation and characterization of cellulose nanofibrils from coconut coir fibers and their reinforcements in biodegradable composite films, Carbohydr Polym. 211 (January) (2019) 49–56. https://linkinghub.elsevier.com/retrieve/pii/S0144861719301067.
[58] H.E. Salama, M.S. Abdel Aziz, Optimized carboxymethyl cellulose and guanidinylated chitosan enriched with titanium oxide nanoparticles of improved UV-barrier properties for the active packaging of green bell pepper, Int. J. Biol. Macromol. 165 (2020) 1187–1197, https://doi.org/10.1016/j.ijbiomac.2020.09.254.
[59] H.A. Karaoglan, N.M. Keklik, N. Develi Isıklı, Degradation kinetics of anthocyanin and physicochemical changes in fermented turnip juice exposed to pulsed UV light,

J. Food Sci. Technol. 56 (1) (2019) 30–39. http://link.springer.com/10.1007/s13197-018-3434-1.
[60] P. Klangmuang, R. Sothornvit, Barrier properties, mechanical properties and antimicrobial activity of hydroxypropyl methylcellulose-based nanocomposite films incorporated with Thai essential oils, Food Hydrocoll. 61 (2016) 609–616, https://doi.org/10.1016/j.foodhyd.2016.06.018.
[61] S.R. Djafari Petroudy, Physical and mechanical properties of natural fibers [Internet], in: Advanced High Strength Natural Fibre Composites in Construction, Elsevier Ltd, 2016, pp. 59–83, https://doi.org/10.1016/B978-0-08-100411-1.00003-0.
[62] J. Chen, H. Li, C. Fang, Y. Cheng, T. Tan, H. Han, Synthesis and structure of carboxymethylcellulose with a high degree of substitution derived from waste disposable paper cups, Carbohydr Polym. 237 (March) (2020), 116040, https://doi.org/10.1016/j.carbpol.2020.116040.
[63] R. Hossain, M. Tajvidi, D. Bousfield, D.J. Gardner, Multi-layer oil-resistant food serving containers made using cellulose nanofiber coated wood flour composites, Carbohydr Polym. 267 (May) (2021), 118221, https://doi.org/10.1016/j.carbpol.2021.118221.
[64] A. Fillat, J. Martínez, C. Valls, O. Cusola, M.B. Roncero, T. Vidal, et al., Bacterial cellulose for increasing barrier properties of paper products, Cellulose 25 (10) (2018) 6093–6105. http://link.springer.com/10.1007/s10570-018-1967-0.
[65] F. Hoeng, J. Bras, E. Gicquel, G. Krosnicki, A. Denneulin, Inkjet printing of nanocellulose-silver ink onto nanocellulose coated cardboard, RSC Adv. 7 (25) (2017) 15372–15381, https://doi.org/10.1039/C6RA23667G.
[66] C. Aulin, M. Gällstedt, T. Lindström, Oxygen and oil barrier properties of microfibrillated cellulose films and coatings, Cellulose 17 (3) (2010) 559–574, https://doi.org/10.1007/s10570-009-9393-y.
[67] L. Dai, Z. Long, J. Chen, X. An, D. Cheng, A. Khan, et al., Robust guar gum/cellulose nanofibrils multilayer films with good barrier properties, ACS Appl. Mater. Interfaces 9 (6) (2017) 5477–5485.
[68] S. Shankar, J.W. Rhim, Antimicrobial wrapping paper coated with a ternary blend of carbohydrates (alginate, carboxymethyl cellulose, carrageenan) and grapefruit seed extract, Carbohydr. Polym. 196 (April) (2018) 92–101, https://doi.org/10.1016/j.carbpol.2018.04.128.
[69] N.R. Saha, G. Sarkar, I. Roy, D. Rana, A. Bhattacharyya, A. Adhikari, et al., Studies on methylcellulose/pectin/montmorillonite nanocomposite films and their application possibilities, Carbohydr. Polym. 136 (2016) 1218–1227, https://doi.org/10.1016/j.carbpol.2015.10.046.
[70] S. Tajik, Y. Maghsoudlou, F. Khodaiyan, S.M. Jafari, M. Ghasemlou, M. Aalami, Soluble soybean polysaccharide: a new carbohydrate to make a biodegradable film for sustainable green packaging, Carbohydr Polym. 97 (2) (2013) 817–824, https://doi.org/10.1016/j.carbpol.2013.05.037.
[71] P. Ezati, R. Priyadarshi, Y.-J. Bang, J.-W. Rhim, CMC and CNF-based intelligent pH-responsive color indicator films integrated with shikonin to monitor fish freshness, Food Control. 126 (1–3) (2021), 108046, https://doi.org/10.1016/j.foodcont.2021.108046.
[72] J. Song, O.J. Rojas, PAPER CHEMISTRY: Approaching super-hydrophobicity from cellulosic materials: a review, Nord Pulp Pap. Res. J. 28 (2) (2013) 216–238. http://www.degruyter.com/view/j/npprj.2013.28.issue-2/npprj-2013-28-02-p216-238/npprj-2013-28-02-p216-238.xml.
[73] E.A. Vogler, Structure and reactivity of water at biomaterial surfaces, Adv Colloid Interface Sci. 74 (1–3) (1998) 69–117. https://linkinghub.elsevier.com/retrieve/pii/S0001868697000407.
[74] M.M.G. de Oliveira, Silva K. de Souza, M.A. Mauro, Evaluation of interactions between carboxymethylcellulose and soy protein isolate and their effects on the preparation and characterization of composite edible films, Food Biophys. 16 (2) (2021) 214–228, https://doi.org/10.1016/j.carbpol.2015.10.046.
[75] B. He, S. Wang, P. Lan, W. Wang, J. Zhu, R. Priyadarshi, et al., Topography and physical properties of carboxymethyl cellulose films assembled with calcium and gelatin at different temperature and humidity, Food Chem. 382 (November 2021) (2020) 229–235, https://doi.org/10.1016/j.ijbiomac.2020.06.155.
[76] K. Chi, J.M. Catchmark, Improved eco-friendly barrier materials based on crystalline nanocellulose/chitosan/carboxymethyl cellulose polyelectrolyte complexes, Food Hydrocoll. 80 (2018) 195–205, https://doi.org/10.1016/j.foodhyd.2018.02.003.
[77] J. Vartiainen, M. Vähä-Nissi, A. Harlin, Biopolymer films and coatings in packaging applications—a review of recent developments, Mater Sci Appl. 05 (10) (2014) 708–718. http://www.scirp.org/journal/doi.aspx?DOI=10.4236/msa.2014.510072.
[78] S. Virtanen, J. Vartianen, H. Setälä, T. Tammelin, S. Vuoti, Modified nanofibrillated cellulose–polyvinyl alcohol films with improved mechanical performance, RSC Adv. 4 (22) (2014) 11343. http://xlink.rsc.org/?DOI=c3ra46287k.
[79] Q. Gao, M. Lei, K. Zhou, X. Liu, S. Wang, H. Li, Preparation of a microfibrillated cellulose/chitosan/polypyrrole film for active food packaging, Prog. Org. Coat. 149 (November 2019) (2020) 105907, https://doi.org/10.1016/j.porgcoat.2020.105907.
[80] H.P. Austin, M.D. Allen, B.S. Donohoe, N.A. Rorrer, F.L. Kearns, R.L. Silveira, et al., Characterization and engineering of a plastic-degrading aromatic polyesterase, Proc. Natl. Acad. Sci. U. S. A. 115 (19) (2018) E4350–E4357.
[81] S. Kane, E. Van Roijen, C. Ryan, S. Miller, Reducing the environmental impacts of plastics while increasing strength: biochar fillers in biodegradable, recycled, and fossil-fuel derived plastics, Compos. Part C Open Access 8 (March) (2022), 100253, https://doi.org/10.1016/j.jcomc.2022.100253.